BNL-102143-2014-TECH
RHIC/AP/32;BNL-102143-2013-IR

Using Small Profile Changes in the Arc Dipoles to Reduce b4 Harmonic Errors

G. F. Dell

June 1994

Collider Accelerator Department
Brookhaven National Laboratory

U.S. Department of Energy
USDOE Office of Science (SC)

DISCLAIMER

Using small profile changes in the arc dipoles to reduce b_4 harmonic errors

G.F. Dell, F. Pilat, and S. Peggs

1. Introduction

Cold measurements on dipole DRG101 indicate b_4'=–1.63 at the 660 Amp excitation needed for injection. This value is outside the estimated range of b_4'[1] and should produce large tuneshifts. A study in which warm measurements from DRG101 and DRG111 were combined and then normalized to the cold measurement on DRG101 at 1450 Amp suggested minor changes in the cross section that should reduce the b_4' magnetic harmonic error[2]. The values of the allowed multipoles used in that study are listed in Table 1 for clarity.

Table 1: Predicted multipoles at 1450 A

scenario	$<b_2'>$	$\Delta<b_2'>$	$<b_4'>$	$\Delta<b_4'>$	$<b_6'>$	$\Delta<b_6'>$	$<b_8'>$	$\Delta<b_8'>$
present	–0.1	0.2	–1.4	0.2	–0.27	0.1	0.28	0.2
phase 1	3	2	–0.4	0.3	0	0.2	0.4	0.1
phase 2	2	2	0	0.5	–0.3	0.2	0.2	0.1

The *"present"* scenario shows estimates for systematic multipoles at 1450A of dipoles having the cross section of DRG101. The *"phase 1"* scenario gives estimated multipoles if the thickness of the midplane cap were reduced from 0.006 inches to 0.004 inches, and *"phase2"* gives estimates with the 0.006 inch midplane cap but with wedge number 2 slightly modified. The Δ's denote the rms value for "present" and confidence level for "phase1" and "phase2" scenarios.

The present note has been written to document the requirements on sextupoles used for chromaticity correction and the tuneshifts from decapole fields associated with the suggested changes. We use $<b_n'>$ to denote the systematic harmonic expected from the magnet design, $\Delta<b_n'>$ to denote the uncertainty in the systematic harmonic resulting from systematic manufacturing errors, and assume $\sigma(b_n')=0$. Hence all multipoles in the Grumman dipoles are treated as being systematic. At injection the magnetic rigidity and chromaticity are small, so sextupole correctors are more than adequate. However, the effects from $<b_4'>$ are expected to be important since the beam size in the arc dipoles is large. At storage the magnetic rigidity is high, and the $\beta^*=1m$ insertions make major contributions to the chromaticity. Requirements on sextupole correctors in the arcs are of concern; especially if operation with as many as four $\beta^*=1m$ insertions is contemplated. On the other hand, the large β functions in the triplet quadrupoles will define the aperture, and the corresponding amplitudes in the arc dipoles will be small. Hence the contributions from $<b_4'>$ are thought to be less important than they are at injection. Consequently we consider in this note the requirements on sextupole correctors from $<b_2'>$ at storage and tuneshifts from $<b_4'>$ at injection. It is assumed that changes in $<b_2'>$ and $<b_4'>$ measured in DRG101 (Table 2) can be used to correct the values listed in Table 1 to 660 A and

5000 A (Table 3 and Table 4) .

Table 2: Straight section multipoles from measurements on DRG101 [3]

	Warm	660 A	1450 A	5000 A	Δ(660-1450)	Δ(5000-1450)
$<b_2'>$	+1.98	-1.20	+0.31	-1.49	-1.51	-1.80
$<b_4'>$	-1.17	-1.63	-1.48	-1.07	-0.15	+0.41

Table 3: Straight section multipoles normalized from DRG101 (660A)

scenario	$<b_2'>$	$\Delta<b_2'>$	$<b_4'>$	$\Delta<b_4'>$
present	−1.61	0.2	−1.55	0.2
phase 1	1.5	2	−0.55	0.3
phase2	0.5	2	−0.15	0.5

Table 4: Straight section multipoles normalized from DRG101 (5000A)

scenario	$<b_2'>$	$\Delta<b_2'>$	$<b_4'>$	$\Delta<b_4'>$
present	-1.9	0.2	−1.0	0.2
phase 1	1.2	2	0.0	0.3
phase 2	0.2	2	0.41	0.5

2. Sextupole requirements at storage

The required integrated sextupole strengths (T/m) have been parametrized with the following relations [4].

$$\left(\frac{d^2B}{dx^2}L\right)_D = -167.2 - 11.021 \times \langle b_2' \rangle - 74.661 \times n^* \qquad (1)$$

$$\left(\frac{d^2B}{dx^2}L\right)_F = 61.01 - 6.03 \times \langle b_2' \rangle + 40.844 \times n^* \qquad (2)$$

where $(d^2B/dx^2\ L)_D$ and $(d^2B/dx^2\ L)_F$ are the integrated sextupole strengths of the SD and SF sextupoles, respectively, and $n^* = \sum\left(\frac{1}{\beta^*}\right)$ is the effective number of $\beta^*=1m$ insertions. The SD sextupoles have the most stringent requirements. At their maximum excitation of 100 A, $(d^2B/dx^2\ L)_D$=-580 T/m. When $<b_2'> = 5$, the example given in [4], the resulting n^* is 4.8. This indicates that there should be sufficient strength to correct a lattice having four

$\beta^*=1m$ and two $\beta^*=2.5m$ insertions.

Equations 1 and 2 were obtained for the baseline lattice with the "expected" systematic multipoles of [1] in the body, lead and nonlead ends of all dipoles and quadrupoles. The measured multipoles from the lead and nonlead ends of DRG101 are different from the "expected" values. A $\Delta\langle b_2'\rangle = \Delta\langle B_2'\rangle / 9.45 = 0.85$ has been added to $\langle b_2'\rangle$ in the body of all 8 cm dipoles; see Table 5 below.

Table 5: Multipoles from lead and nonlead ends of 8cm dipoles; $\Delta(b_2') = \Delta(B_2')/9.45$

	"expected"	DRG101	$\Delta(B_2')$	$\Delta(b_2')$
B_2' (lead)	21	22.8	+1.8	+0.19
B_2' (nonlead)	1	5.2	+6.2	+0.66

The required strength of the SD sextupoles increases as $\langle b_2'\rangle$ becomes increasingly positive. The positive sign of the uncertainty of $\langle b_2'\rangle$ in Table 4 is selected to require the greatest SD strength, and n^* is determined using the relation $n^* = 5.529 - 0.1476\ \langle b_2'\rangle$ that is obtained from Eq.1 when $(d^2B/dx^2\ L)_D = -580\ T/m$. The results for the three scenarios are listed in Table 6.

Table 6: Total b_2 and resulting n^*

Scenario	$\langle b_2'\rangle$ *(total)*	n^*
present	-1.9 + 0.2 + 0.85 = -0.85	5.65
phase 1	+1.2 + 2.0 + 0.85 = 4.05	4.93
phase 2	+0.2 + 2.0 + 0.85 = 3.05	5.07

All three scenarios are less demanding than that represented by $\langle b_2'\rangle = 5$ used in [4]. Perhaps of more interest is the integrated sextupole strength and the required current [5] for operation with two $\beta^* = 1m$ insertions and four at $\beta^* = 10m$ ($n^*= 2.4$) or operation with four $\beta^* = 1m$ and two $\beta^* = 10m$ ($n^*= 4.2$), as shown in Table 7. We conclude that systematic b_2' from dipole cross sections place no limit on chromaticity correction at storage for all the scenarios 1 to 3

Table 7: Predicted sextupole requirements at 5000 A

		$2 * \beta^* = 1m$		$4 * \beta^* = 1m$	
scenario	$\langle b_2'\rangle$	$(BL)_D$	I (A)	$(BL)_D$	I (A)
present	-0.85	–337	–38.24	–471.4	–64.25
phase 1	4.05	–391	–46.11	–525.4	–81.18
phase 2	3.05	–380	–44.41	–514.4	–77.66

3. Impact of systematic b_4' at injection

The primary concern about $\langle b_4'\rangle$occurs at injection where the beam in the arc dipoles is large. Dependence of tune

on amplitude and aspect ratio x/y has been determined at $\Delta p/p = 0$ and $+/- 0.11$ % using the baseline lattice and baseline multipoles in all elements except the 8cm dipoles. In these elements all multipoles except $<b_2'>$ and $<b_4'>$ have baseline values, while $<b_2'>$ and $<b_4'>$ have values listed in Table 3. Tune determinations were made using two different sets of randomly generated errors. However, for the baseline lattice, randomness is limited to rms position errors of 0.5mm, rms rolls of one mrad, and $\sigma a_1'$ and $\sigma b_1'$ in all dipoles and quadrupoles. Results from the two seeds are nearly identical, so results from seed 0 only are shown.

At injection $\beta^*=10$ *m*, the normalized emittance corresponding to $(6)^{1/2}\sigma$ is $\varepsilon_o=10$ (π mm mrad), the total energy $E = 12$ *GeV*, $\gamma = 12.89$, and $\sigma = 1.1389$*mm*. Tracking was performed with initial total action $\varepsilon_{tot} = (n^*\sigma)^2/\beta^*$ with n = 2, 4, 6 and 7. Figure 1 shows four tuneleaf plots: the baseline lattice (lower left), scenario 1 (upper left), scenario 2 (upper right), and scenario 3 (lower right). The most obvious feature is the off momentum leafs in the plot for scenario 1. It is known that the tuneshift from b_4' has an antisymmetric dependence on $\Delta p/p$ and adds constructively to the baseline tuneshift at one extreme of $\Delta p/p$ and destructively at the other extreme of $\Delta p/p$. The constructive addition pushes the tune towards the coupling and sixth order resonances, while the destructive addition reduces the overall tunespread and may be too small for stability. Based on Figure 1 and the rather modest range of initial action, both scenario's 2 and 3 are acceptable with scenario 3 having more complete cancellation of $<b_4'>$ from body and ends. However results based on two dipoles, one of which is known to have incorrectly sized coils (DRG111), should not be considered irrefutable.

4. Studies from tracking on a uniform grid in a_x, a_y space

The dynamics for the 3 scenarios has been studied also with tracking performed in amplitude space. Initial conditions for particles are generated on a regular rectangular grid (a_x, a_y), the particle trajectories are tracked and the linear aperture is studied by calculating the tune and the smear. The smears are defined as follows:

horizontal smear $\qquad S_{xx} = \sqrt{\sigma_{xx}} \qquad \sigma_{xx} = \dfrac{\langle a_x^2 \rangle}{\langle a_x \rangle^2} - 1$

vertical smear $\qquad S_{yy} = \sqrt{\sigma_{yy}} \qquad \sigma_{yy} = \dfrac{\langle a_y^2 \rangle}{\langle a_y \rangle^2} - 1$

correlation smear $\qquad \sigma_{xy} = \dfrac{\langle a_x a_y \rangle}{\langle a_x \rangle \langle a_y \rangle} - 1$

The smears and the tunes are subsequently plotted as 3D surfaces and contours on the grid of initial amplitudes. The program also finds the resonance lines that affect the particular area of phase space defined by the grid.
For the present study of the effect of $<b_2'>$ and $<b_4'>$multipoles we selected a grid ($12\sigma_x$, $12\sigma_y$) where particles are generated with x amplitudes increasing from 0 to $12\sigma_x$ by $\Delta=0.5\sigma_x$, and respectively with y amplitudes from 0 to $12\sigma_y$ by $\Delta=0.5\sigma_y$. The initial conditions span an area in phase space sufficient to observe particle losses for the larger amplitudes. (When a particle is lost, the smears are by convention set to zero and the tunes set to the nominal tune). The 576 particles are tracked for 256 turns, a reasonable compromise between accuracy and tracking time.
Tune and smear plots were produced for Scenario 1, the "present" or do-nothing scenario, for Scenario 2, reduction of the midplane cap thickness and for Scenario 3, modification of wedge #2. Each run, on momentum and off momentum by $\Delta p/p$=+0.11% and $\Delta p/p$=-0.011% corresponds to one of the tune "leaves" shown in Figure 1, in that the error configuration of the machine is the same, although the phase space area spanned is different. The analysis was

repeated for 2 seeds but only the results concerning seed 0 will be described here since the differences between seeds, as already remarked, are minimal.
Figure 2a, 3a and 4a contain the smear plot surfaces for Scenario 1 for $\Delta p/p$=+0.11%, $\Delta p/p$=0 and $\Delta p/p$=–0.11% respectively; the corresponding contour plots (Figure 2b, 3b and 4b) are also shown together with the coupling resonance. It can be noticed that the phase space area affected by the coupling resonance also exhibits large smear variations. The largest effect on the smears happens for $\Delta p/p$=-0.11% when a relatively large area of phase space is affected by the coupling resonance. That is in accordance with the results obtained for the tunes in Figure 1 (upper left plot) where the larger amplitudes appear to approach the coupling resonance.
Figure 5a and 5b, 6a and 6b describe respectively Scenario 2 and 3 for the case $\Delta p/p$=–0.11%: the linear aperture is improved with respect to Scenario 1 in both cases, and the differences between Scenario 2 and 3 are marginal, also this in accordance with the results obtained in the tune space.
A comparison between the horizontal smear and the region of (a_x,a_y) space used to generate tuneleaf plots is shown in Figure 2c, where lines of equal smear are broken and lines used for the tracking grid are solid. Also shown is the aperture determined with 1 million turn tracking runs using initial coordinates corresponding to equal action in the horizontal and vertical planes. The aperture limit of 12σ, where $\varepsilon_{tot}=(12\sigma)^2/\beta^*$ is located at the edge of the region where lines of equal horizontal smear become irregular. The lines of equal smear and the radial lines of the grid used to generate the tuneleaf plots are roughly parallel. The fact that small amplitude particles have large smear is thought to result from the normalization used in the smear functions. The current smear plots compare regions where smears are simple functions of the amplitudes and nonlinear phase space regions where the smears are more complicated.

5. New dipoles

Currently five dipoles, DRG101, DRG102, DRG103, DRG104, and DRG111, have been received. Warm measurements supplied by Grumman list average values $\langle b_2'(W)\rangle$ =3.20 and $\langle b_4'(W)\rangle$ =–0.75. Using Table 3 and Table 4 to adjust warm multipoles to 660 and 5000Amps, one obtains the anticipated average multipoles listed in Table 8. The $\langle b_2'\rangle$ is small at injection and storage. The $\langle b_4'\rangle$ lies between the "present" and "phase1" values and should produce tune spreads between that of scenario 1 and scenario 2 in Figure 1.

Table 8: Average body multipoles for 5 dipoles. Warm measurements converted to 5000 A with DRG101 data.

	660 A	5000 A
<b2'>	+0.02	–0.27
<b4'>	–1.21	–0.65

6. Conclusion

The tuneleaf and smear plots indicate that tuneshifts and smears from Scenario 1 (called "Present" in Ref[1]) may be unacceptably large at dp/p=+0.11%. Either Scheme 1 (Scenario 2) in which the midplane cap is reduced by from 0.006" to 0.004" or Scheme 2 (Scenario 3) in which only wedge #2 is changed, produce tune dependence similar to that shown for the baseline lattice. Either of the latter two solutions give acceptable results. The selection should therefore be based on different considerations.

Bibliography

[1]R.Gupta, RHIC-MD-237, May 27, 1994

[2]"Multipole Tables: EXPECTED-Q8.TABLE1-D, EXPECTED-Q13.TABLE2-D, EXPECTED-D8.TABLE3-D, EXPECTED-D10.TABLE4-D,

EXPECTED-D20.TABLE5-D", Magnet Div.,October-November, 1993

[3]"Body and End Harmonics in magnet DRG101", Magnet Division, BODYEND.XLS, December 5, 1994

[4] G.F.Dell and S. Peggs, RHIC/AP/21, March 11, 1994

[5] "Summary of integral T.F. in SRE Magnets", Magnet Division, SRETF-SMY.XLS, February 17, 1994

FIGURE CAPTIONS

Figure 1. Tuneleaf plots showing dependence of tune on amplitude, x-y profile, and momentum error dp/p for several values of b2′ and b4′ errors in the arc dipoles. Seed_0.

a). Baseline multipoles: b2′=-3.5, b4′=0.2
b). Scenario #1: drg101 as is; b2′=-1.6, b4′=-1.5
c). Scenario #2: 0.004 cap, b2′=1.5, b4′=-0.5
d). Scenario #3: change #2 wedge, b2′=0.5, b4′=-0.1

Figure 2(a) Scenario #1: 3D profiles of x, y, and correlation smears for Seed_0 at dp/p=+0.11%

Figure 2(b) Contour plots of x, y, and correlation smears plus coupling resonance. Projection of Figure 2(a) on Ax, Ay plane.

Figure 2(c) Overlay of contour plot of horizontal smear in Figure 2(b) and triangular grid used for tuneleaf generation. Also shown is aperture from one million turn tracking runs made on baseline lattice at dp/p=+0.11% for Seed_1.

Figure 3(a) Scenario #1: 3D profiles of x, y, and correlation smears for Seed_0 at dp/p=+0.0%

Figure 3(b) Contour plots of x, y, and correlation smears plus coupling resonance. Projection of Figure 3(a) on Ax, Ay plane.

Figure 4(a) Scenario #1: 3D profiles of x, y, and correlation smears for Seed_0 at dp/p=-0.11%

Figure 4(b) Contour plots of x, y, and correlation smears plus coupling resonance. Projection of Figure 4(a) on Ax, Ay plane.

Figure 5(a) Scenario #2: 3D profiles of x, y, and correlation smears for Seed_0 at dp/p=-0.11%

Figure 5(b) Contour plots of x, y, and correlation smears plus coupling resonance. Projection of Figure 5(a) on Ax, Ay plane.

Figure 6(a) Scenario #3: 3D profiles of x, y, and correlation smears for Seed_0 at dp/p=-0.11%

Figure 6(b) Contour plots of x, y, and correlation smears plus coupling resonance. Projection of Figure 6(a) on Ax, Ay plane.

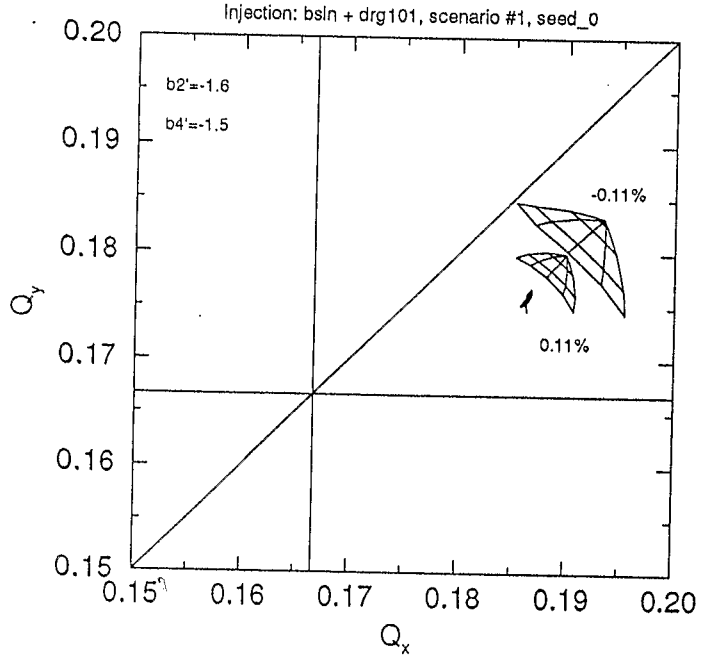

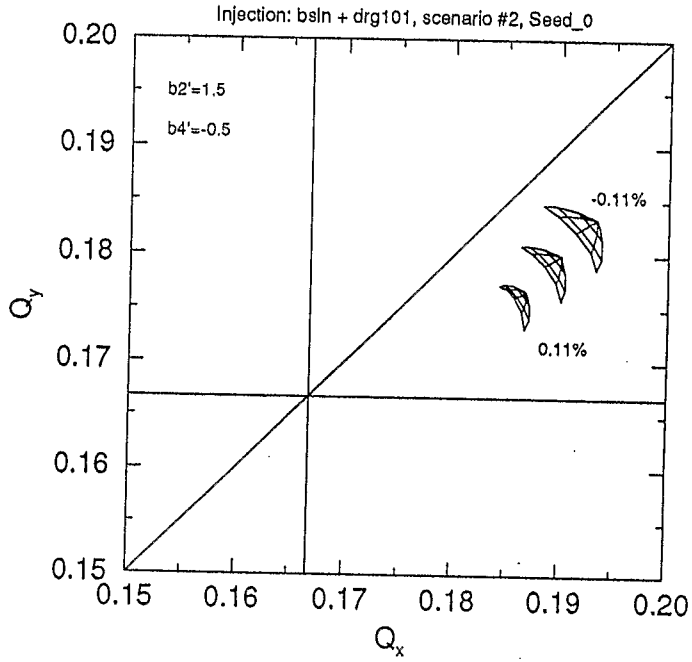

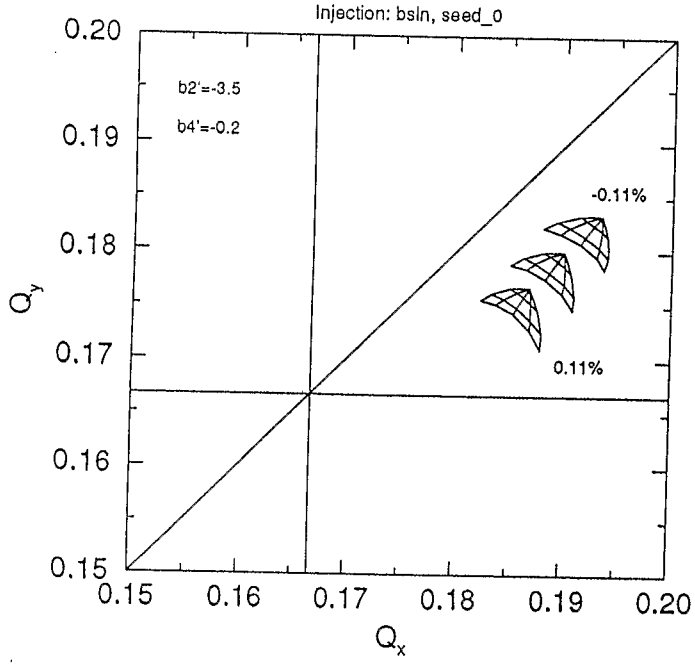

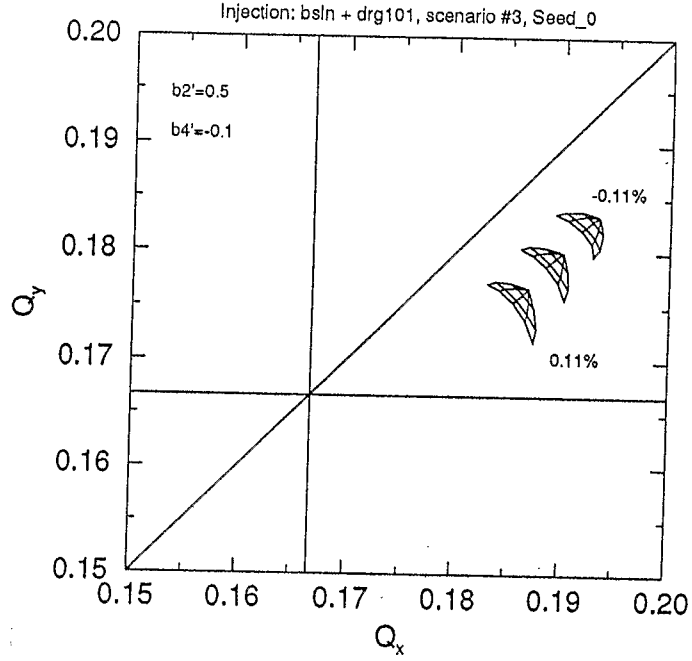

Figure 1 Tunleaf plots for baseline, scenario #1, scenario #2, and scenario #3 configurations

Figure2. **Present: no dipole modification**

injection optics $\Delta p/p = +0.0011$

tracking parameters

grid	x	A_x	$0 \rightarrow 12\sigma_x$	$\Delta=0.5\sigma_x$
	y	Ay	$0 \rightarrow 12\sigma_y$	$\Delta=0.5\sigma_y$

turns 256 particles 576

baseline errors except systematic b2 and b4 in the dipole
(body harmonics)

Horizontal Smear

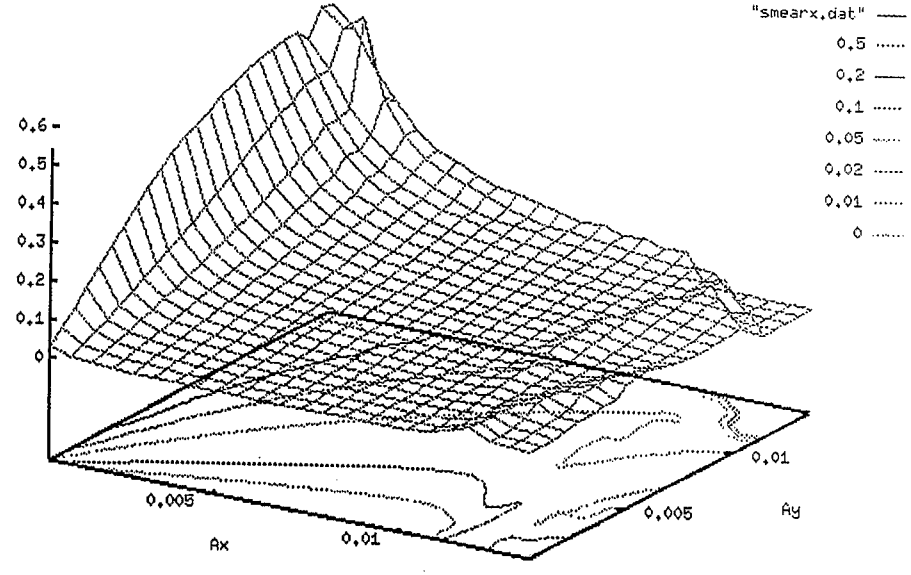

Vertical Smear

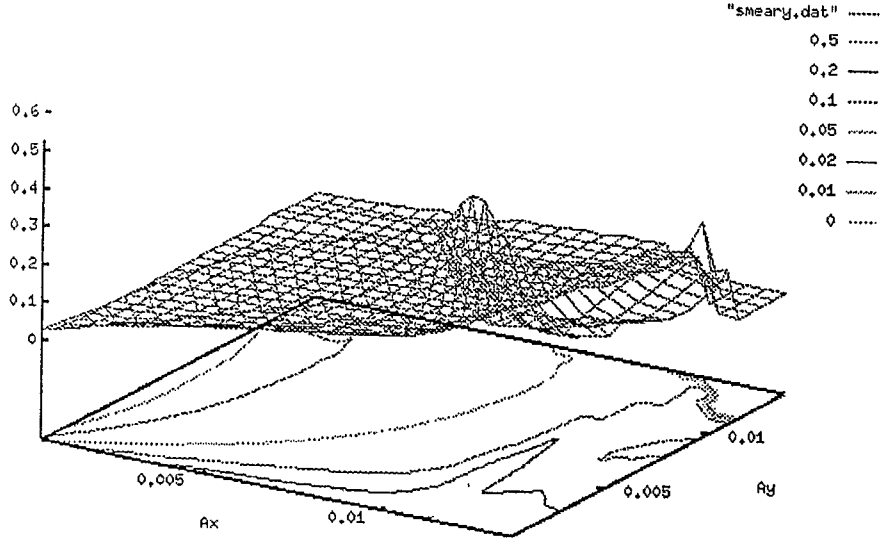

Correlation Smear

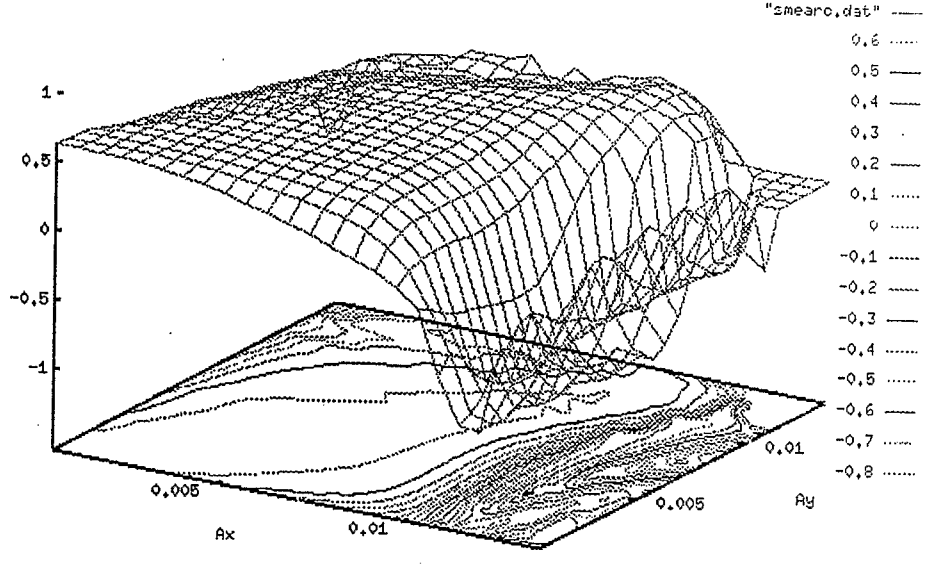

Figure 2(a) 3D plots of smear in Ax, Ay space Scenario #1 at dp/p=+0.11%

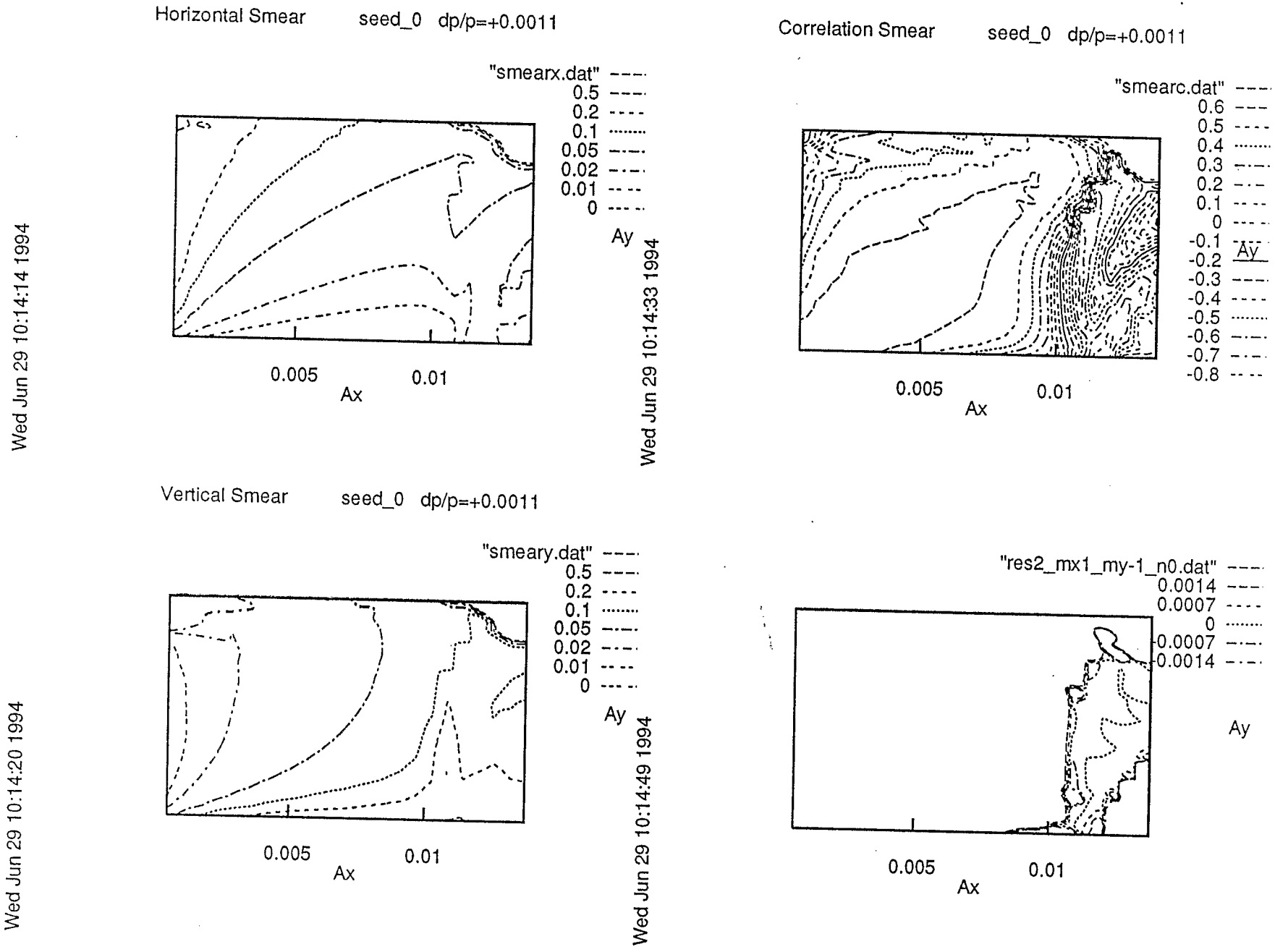

Figure 2(b) Contour plots of smear in Ax, Ay space Scenario #1 at dp/p=+0.11%

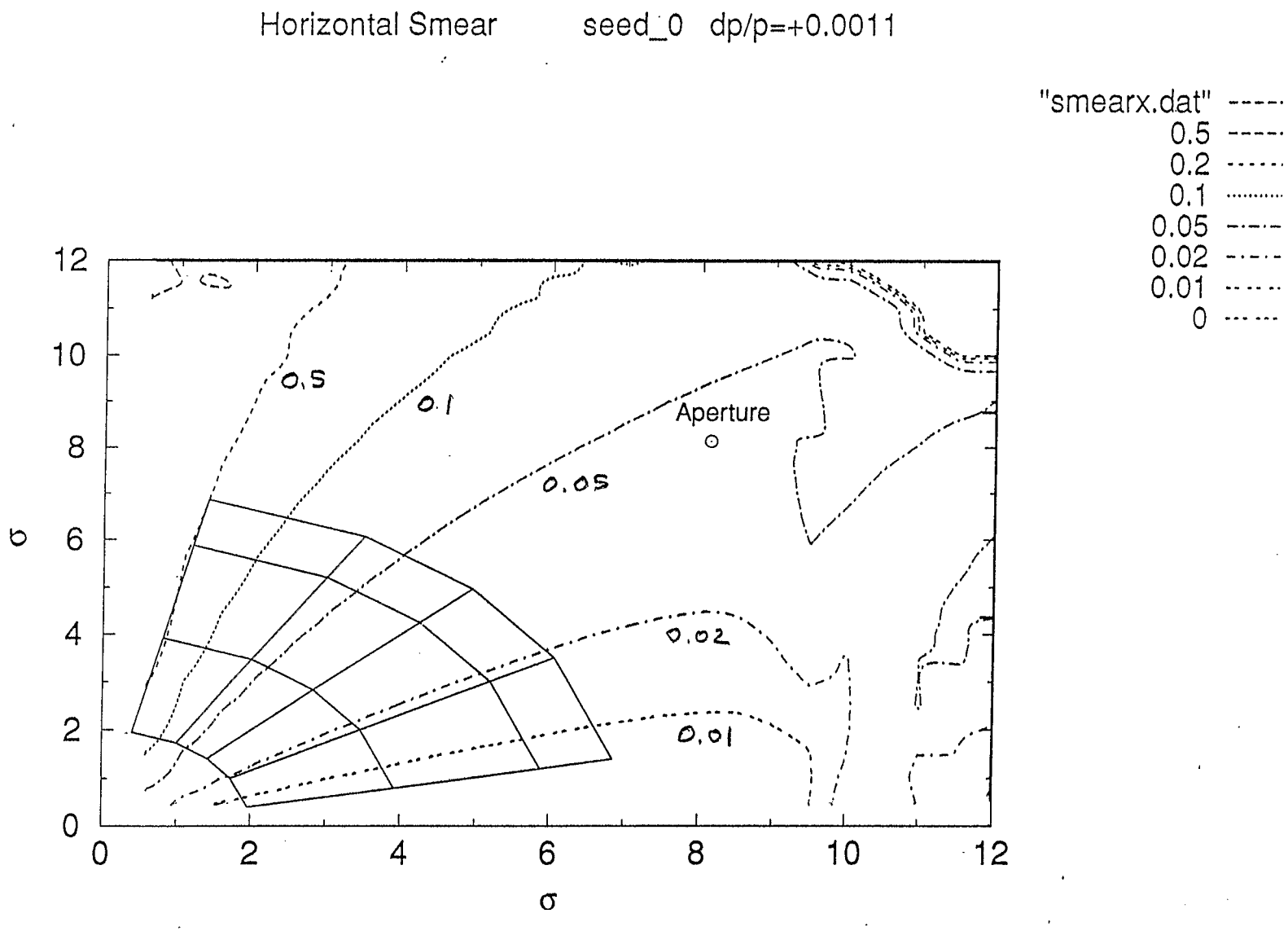

Figure 2(c) Superposition of tuneleaf grid on smear.x contour plot of Figure 2(b)

Figure3. Present: no dipole modification

injection optics $\Delta p/p = 0$

tracking parameters

grid	x	A_x	$0 \rightarrow 12\sigma_x$	$\Delta=0.5\sigma_x$
	y	Ay	$0 \rightarrow 12\sigma_y$	$\Delta=0.5\sigma_y$

turns 256 particles 576

baseline errors except systematic b2 and b4 in the dipole
(body harmonics)

Horizontal Smear

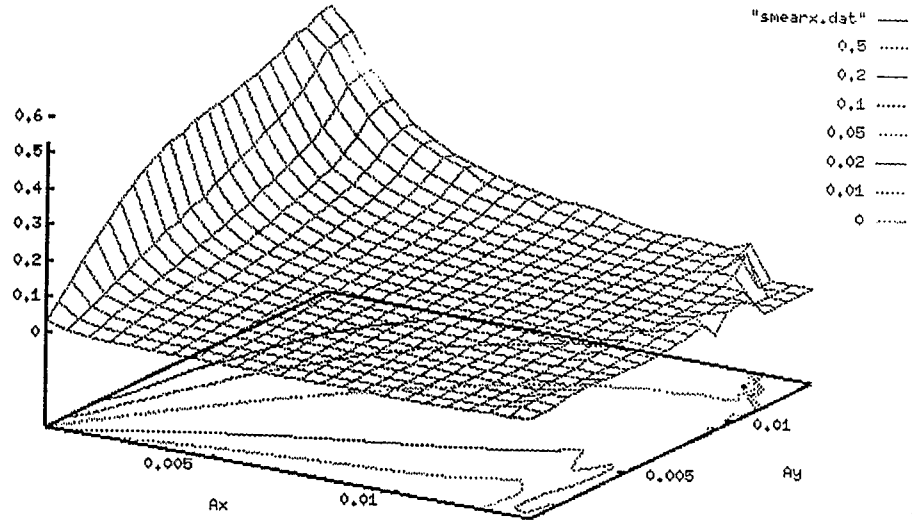

Vertical Smear

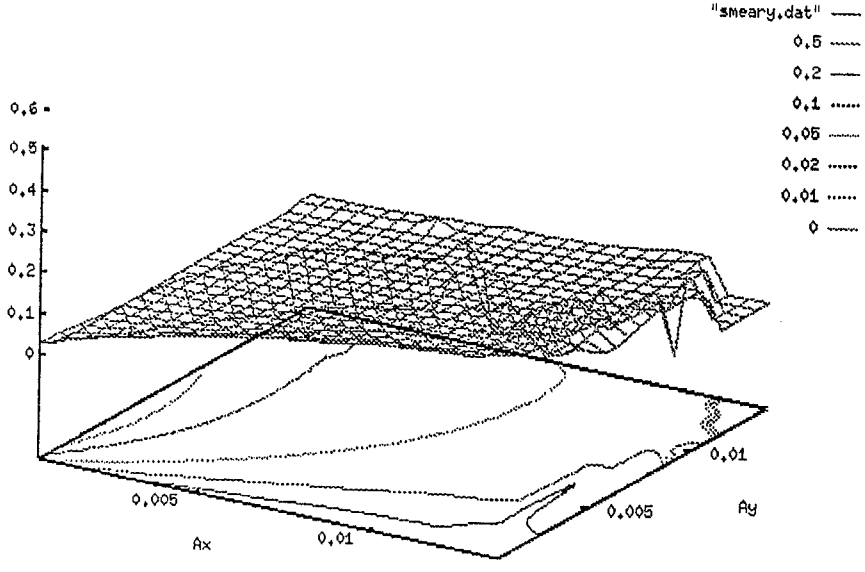

Correlation Smear

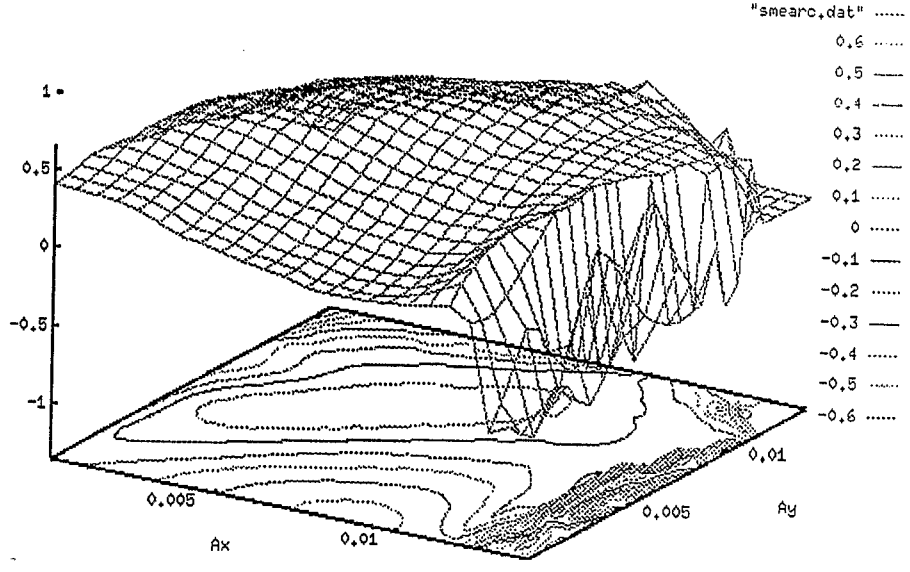

Figure 3(a) 3D plots of smear in Ax, Ay space Scenario #1 at dp/p=+0.0%

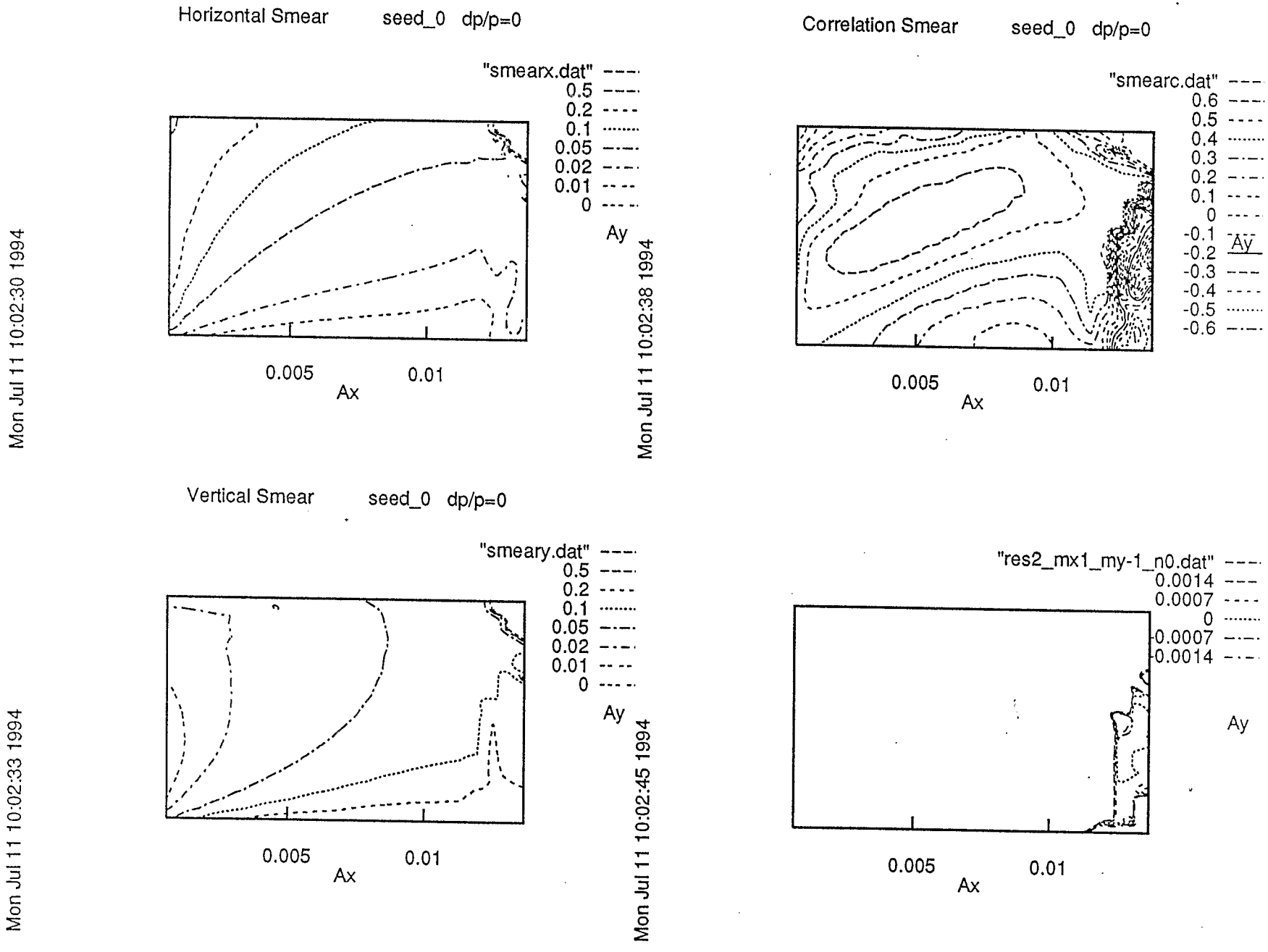

Figure 3(b) Contour plots of smear in Ax, Ay space Scenario #1 at dp/p=+0.0%

Figure 4. Present: no dipole modification

injection optics $\Delta p/p = -0.0011$

tracking parameters

grid	x	A_x	0 --> $12\sigma_x$	$\Delta=0.5\sigma_x$
	y	Ay	0 --> $12\sigma_y$	$\Delta=0.5\sigma_y$

turns 256 particles 576

baseline errors except systematic b2 and b4 in the dipole
(body harmonics)

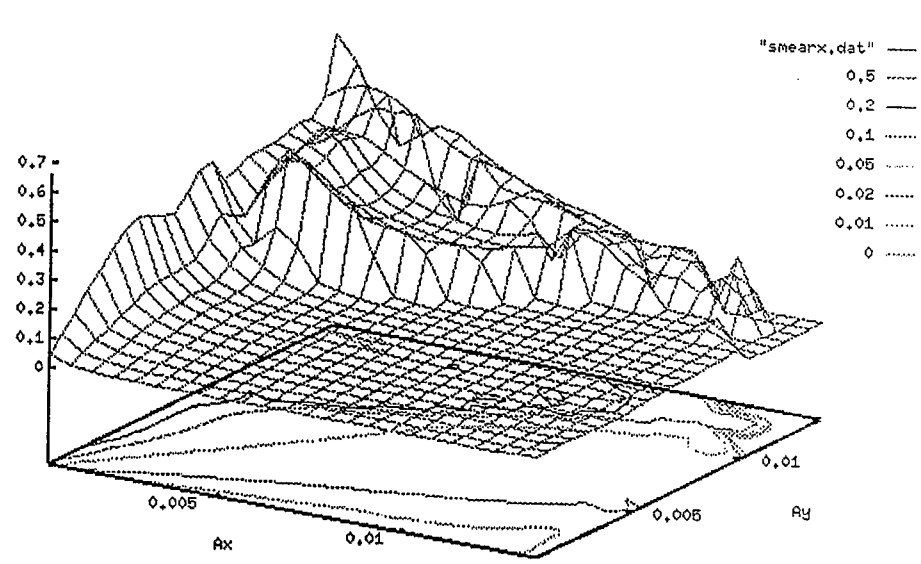

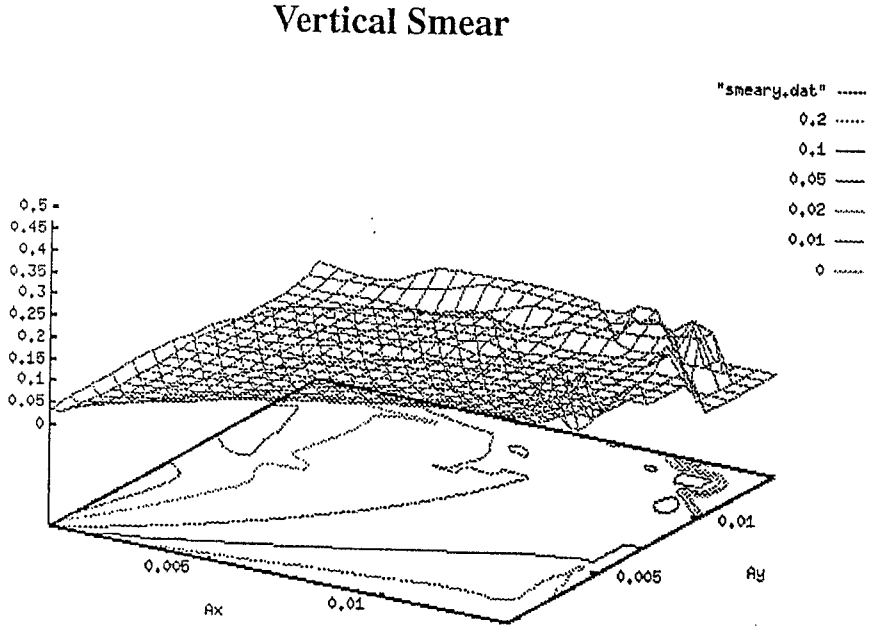

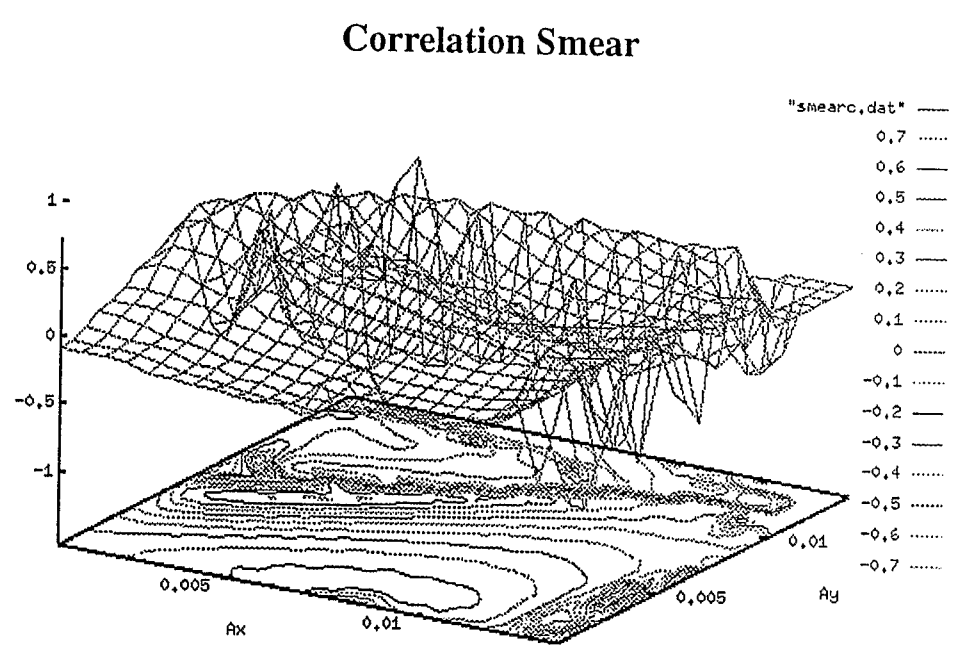

Figure 4(a) 3D plots of smear in Ax, Ay space Scenario #1 at dp/p=-0.11%

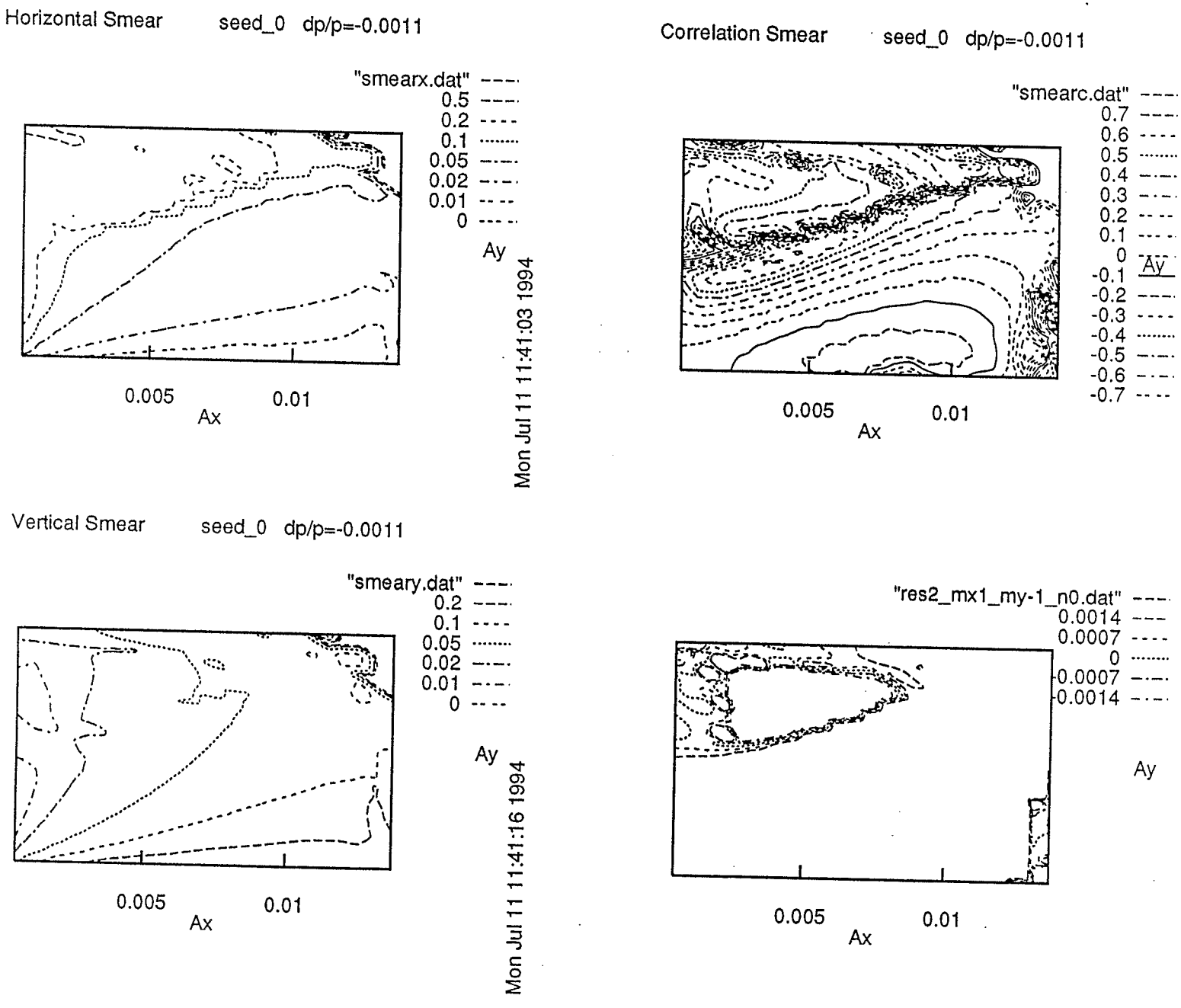

Figure 4(b) Contour plots of smear in Ax, Ay space Scenario #1 at dp/p=-0.11%

Figure 5. Phase 1: modification of midplane cap

injection optics $\Delta p/p = -0.0011$

tracking parameters

grid	x	A_x	$0 \rightarrow 12\sigma_x$	$\Delta=0.5\sigma_x$
	y	Ay	$0 \rightarrow 12\sigma_y$	$\Delta=0.5\sigma_y$

turns 256 particles 576

baseline errors except systematic b2 and b4 in the dipole
(body harmonics)

Horizontal Smear

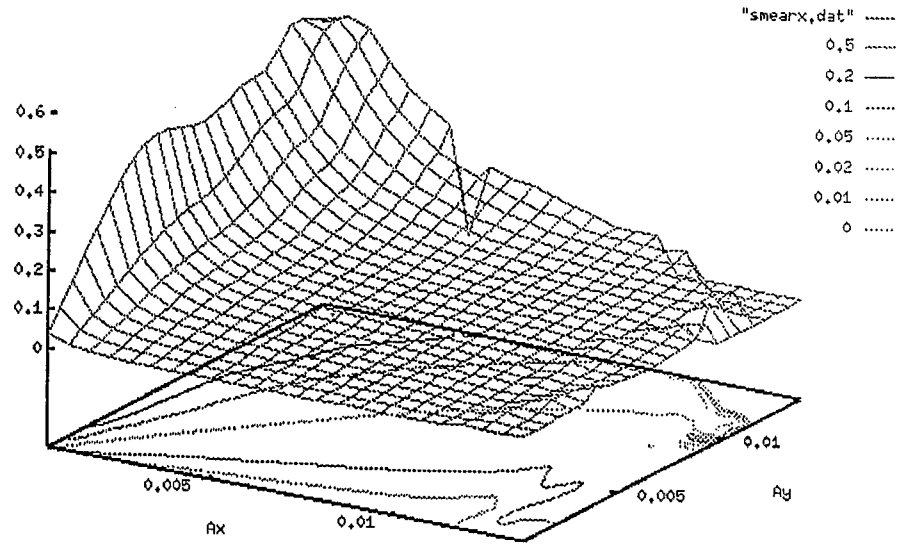

Vertical Smear

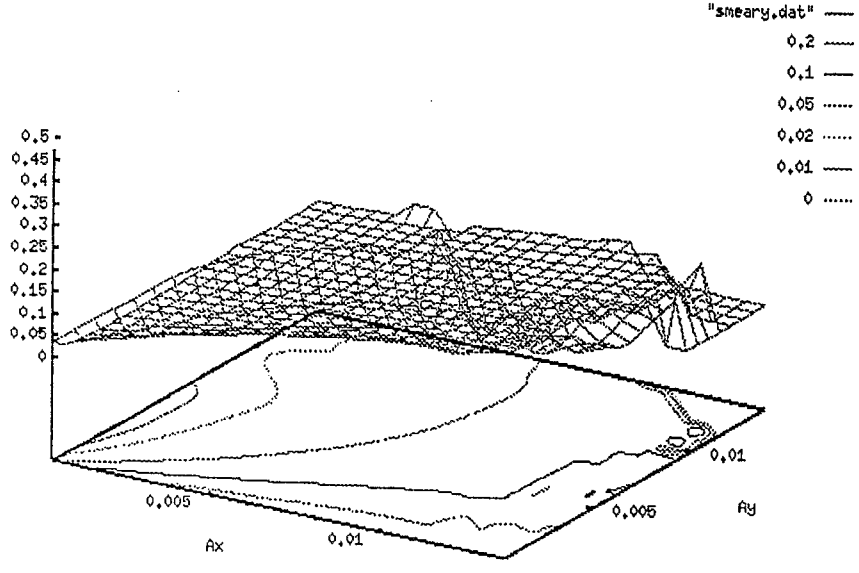

Correlation Smear

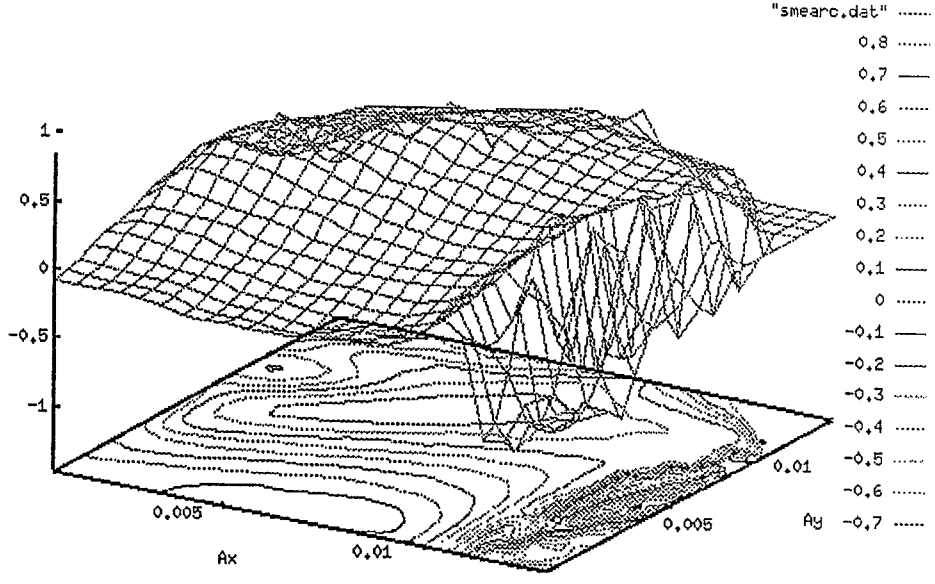

Figure 5(a) 3D plots of smear in Ax, Ay space Scenario #2 at dp/p=-0.11%

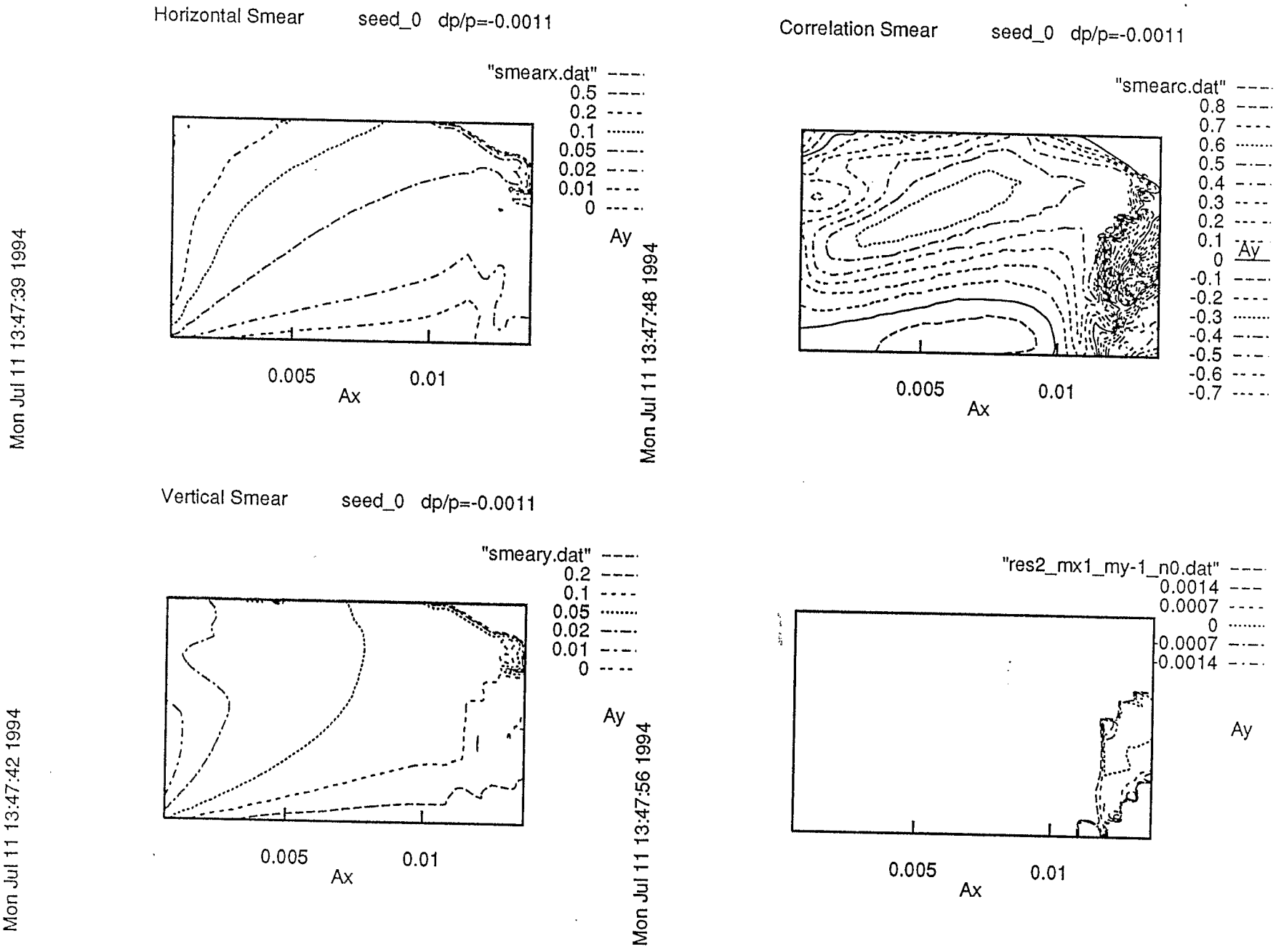

Figure 5(b) Contour plots of smear in Ax, Ay space Scenario #2 at dp/p=-0.11%

Figure 6. Phase 2: modification of wedge 2

injection optics $\Delta p/p = -0.0011$

tracking parameters

grid	x	A_x	$0 \rightarrow 12\sigma_x$	$\Delta=0.5\sigma_x$
	y	Ay	$0 \rightarrow 12\sigma_y$	$\Delta=0.5\sigma_y$

turns 256 particles 576

baseline errors except systematic b2 and b4 in the dipole
(body harmonics)

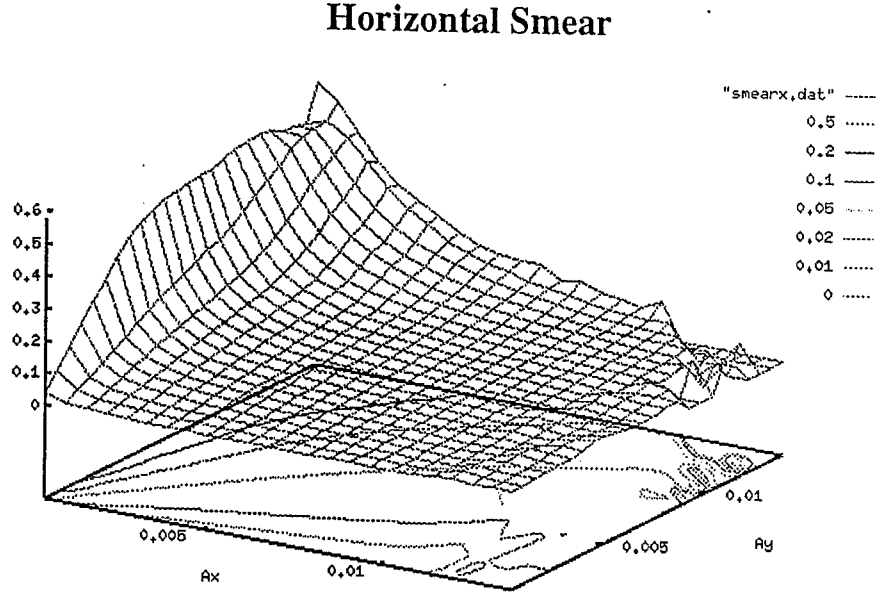

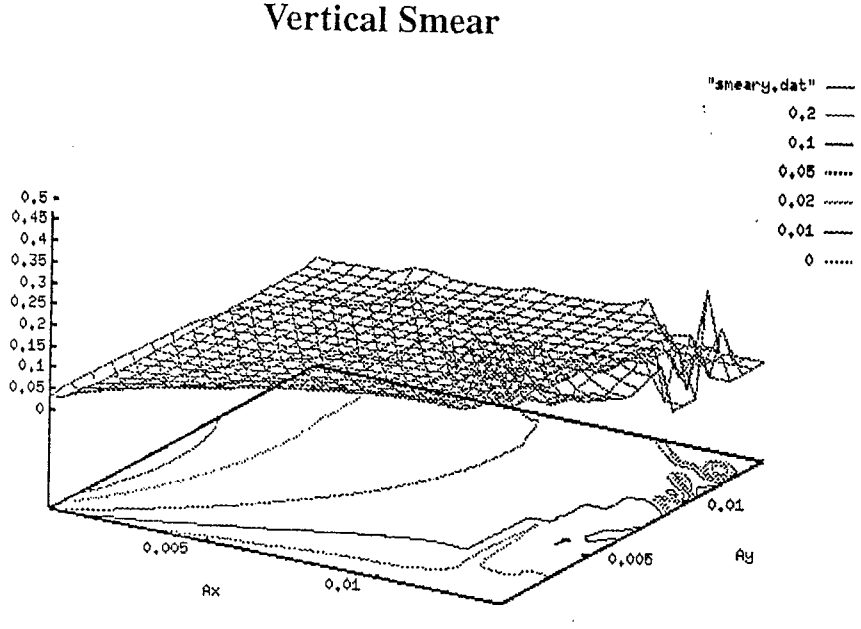

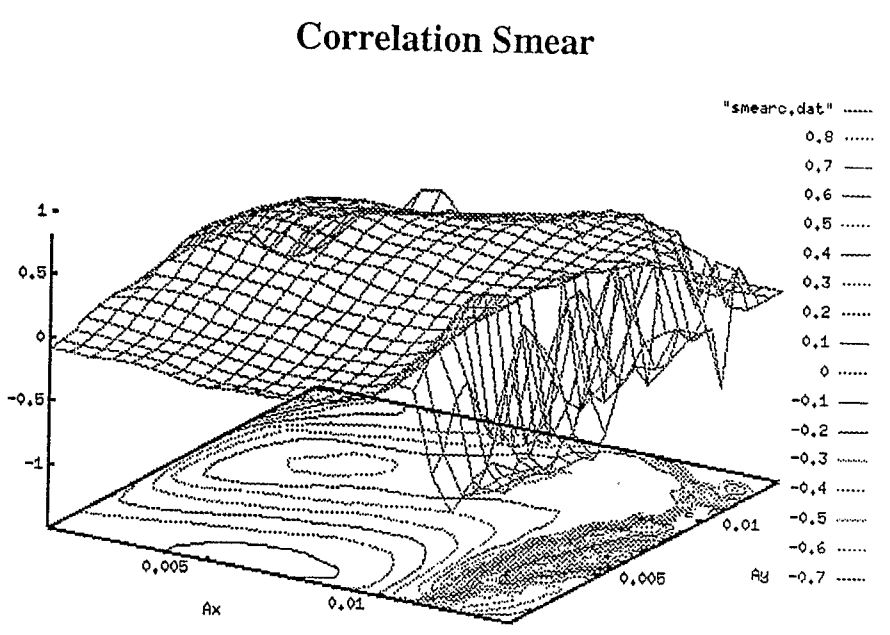

Figure 6(a) 3D plots of smear in Ax, Ay space Scenario #3 at dp/p=-0.11%

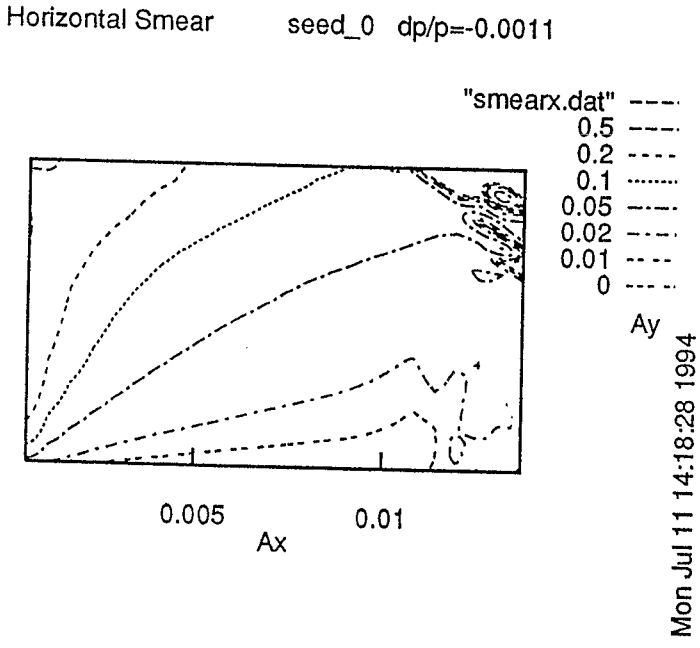

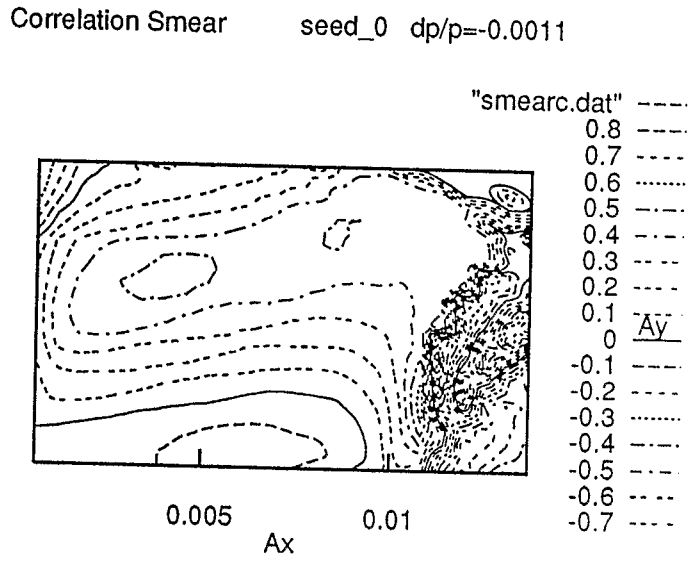

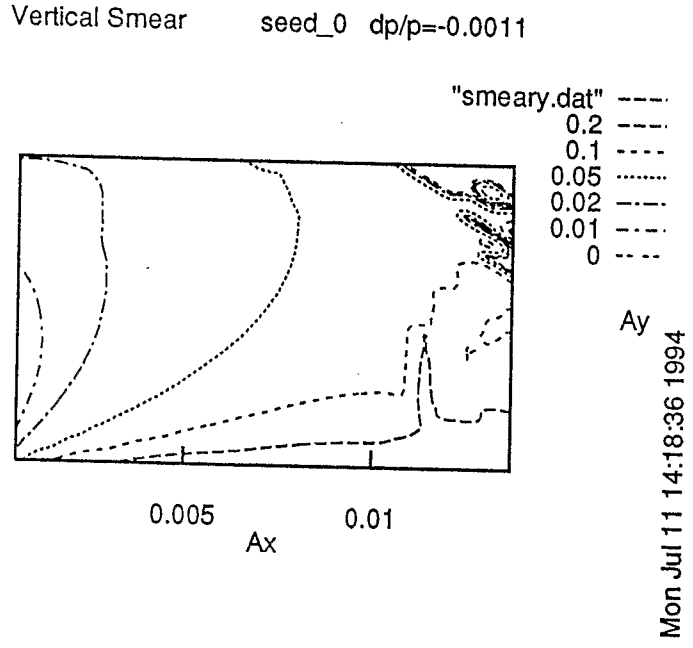

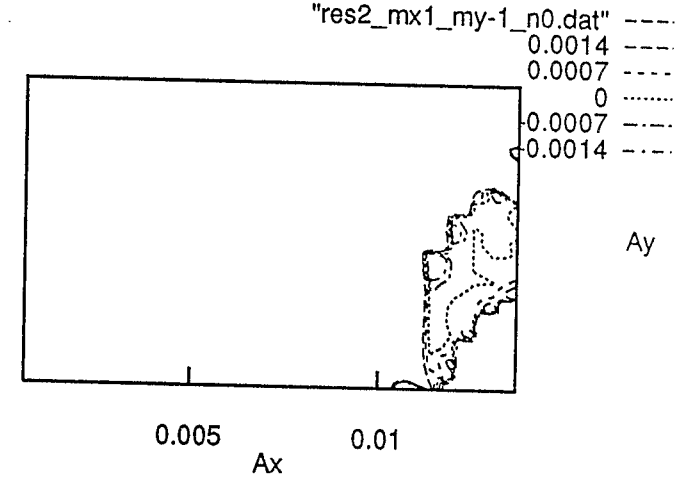

Figure 6(b) Contour plots of smear in Ax, Ay space Scenario #3 at dp/p=-0.11%